THE EVOLVING SIGMOID: EVIDENCE FOR MAGNETIC FLUX ROPES IN THE CORONA BEFORE, DURING, AND AFTER CMES

S. E. GIBSON[1,*], Y. FAN[1], T. TÖRÖK[2] and B. KLIEM[3]
[1]*NCAR/HAO, P.O. Box 3000, Boulder, CO 80301, U.S.A.*
[2]*Mullard Space Science Laboratory, University College London, Holmbury St. Mary, Dorking, Surrey RH5 6NT, U.K.*
[3]*Astrophysical Institute Potsdam, An der Sternwarte 16, 14482 Potsdam, Germany*
*(*Author for correspondence: E-mail: sgibson@ucar.edu)*

(Received 7 July 2005; Accepted in final form 6 February 2006)

Abstract. It is generally accepted that the energy that drives coronal mass ejections (CMEs) is magnetic in origin. Sheared and twisted coronal fields can store free magnetic energy which ultimately is released in the CME. We explore the possibility of the specific magnetic configuration of a magnetic flux rope of field lines that twist about an axial field line. The flux rope model predicts coronal observables, including heating along forward or inverse S-shaped, or sigmoid, topological surfaces. Therefore, studying the observed evolution of such sigmoids prior to, during, and after the CME gives us crucial insight into the physics of coronal storage and release of magnetic energy. In particular, we consider (1) soft-X-ray sigmoids, both transient and persistent; (2) The formation of a current sheet and cusp-shaped post-flare loops below the CME; (3) Reappearance of sigmoids after CMEs; (4) Partially erupting filaments; (5) Magnetic cloud observations of filament material.

Keywords: coronal mass ejections, flares, sigmoids

1. Introduction: The Magnetic Flux Rope Paradigm

We define a magnetic flux rope as a set of magnetic field lines that wind more than once about some common axial field line. Figure 1 shows a picture of the so-called “Granddaddy” prominence which exhibits apparently twisted structure, next to a cartoon showing two views of a flux rope magnetic field line twisting about a straight axis (note that the axial field line does not in general have to be straight). Magnetic flux rope models have been employed to explain a wide range of solar and heliospheric physics phenomena, from the solar interior out into interplanetary space. In particular, a range of CME and CME-associated phenomena have been modeled with magnetic flux ropes. This is not surprising, because the energy source for CMEs is widely agreed to lie in their twisted or sheared magnetic fields. Although coronal magnetic fields are not yet commonly observed, observations of photospheric vector magnetic fields have long shown that non-potential magnetic fields are common (Hagyard, 1984; Tanaka, 1991; Leka *et al.*, 1996; Lites *et al.*, 1995), and observations such as the twisted prominence of Figure 1 indicate that the coronal field tied to the plasma is likewise significantly non-potential. Twisted magnetic flux ropes are good candidates for metastable coronal MHD equilibria

Space Science Reviews (2006) 124: 131–144
DOI: 10.1007/s11214-006-9101-2

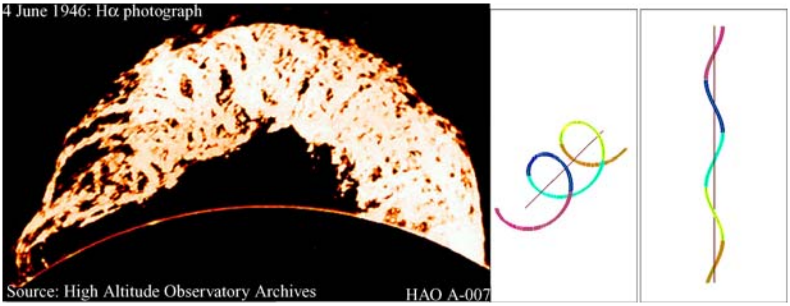

Figure 1. (Left) The "Granddaddy" prominence (HAO H-alpha), (right) two views of flux rope cartoon, demonstrating that a single twisted field line (in this case, left-handed) includes both forward and inverse S shapes.

capable of storing free magnetic energy which may be tapped to drive coronal dynamic phenomena such as CMEs (Low, 1996; Rust, 2003).

CMEs have been related to interplanetary counterparts, such as magnetic clouds, which are well-modeled as magnetic flux ropes (Burlaga *et al.*, 1982). The idea of the CME as a magnetic flux rope has gained acceptance over the years, and a brief survey of recent CME model publications shows that they are united in describing the erupting CME as a flux rope (Amari *et al.*, 2003a,b; Chen and Krall, 2003; Roussev *et al.*, 2003; MacNeice *et al.*, 2004; Manchester *et al.*, 2004a). However, the question of whether the flux rope is formed during the eruption, or whether the flux rope existed prior to the eruption, remains controversial. In this paper we will argue for the existence of a stable, pre-CME magnetic flux rope, by showing that models of this type can explain the observed evolution of soft-X-ray sigmoids in relation to CMEs and filament eruptions.

2. Sigmoids

2.1. Sigmoid Observations

Sigmoids are forward or inverse S-shaped structures observed in the solar corona. Active regions possessing sigmoids have been shown to be significantly more likely to produce flares or CMEs than non-sigmoid active regions (Canfield *et al.*, 2000). Sigmoids can be classified as transient or persistent. Persistent sigmoids can be a collection of sheared loops that together indicate an S or inverse-S shape for days or weeks, while transient sigmoids tend to be more sharply focussed into apparently a single, sigmoid loop, and can appear and disappear multiple times during their disk passage (Pevtsov, 2002b). Transient sigmoids are often associated with a CME, and in such cases may transition into post-flare cusped loops. Figure 2 gives examples of a variety of sigmoids. Sigmoids are generally observed in soft-X-ray emission, but can be visibile in UV or EUV, particularly transient sigmoids

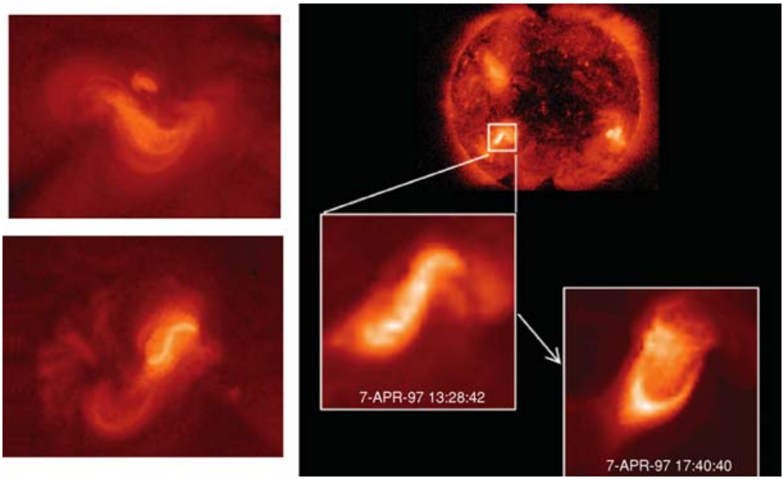

Figure 2. Examples of soft-X-ray sigmoids, as observed by Yohkoh SXT. (left top) Persistent sigmoid; (left bottom) transient sigmoid; (right) sigmoid associated with CME, transitioning to cusp.

(Sterling and Hudson, 1997; Gibson *et al.*, 2002). Forward or inverse S-shaped filaments also can be visible in H-alpha along a neutral line in sigmoid active regions (Rust and Kumar, 1994; Pevtsov *et al.*, 1996; Lites and Low, 1997; Gibson *et al.*, 2002). Even after CMEs and sigmoid-to-cusp transitions, active regions can exhibit sigmoid structures again within a matter of hours. Likewise, a sigmoid filament can also reform after an eruption, or even sometimes appear unaffected altogether by the flare/CME/sigmoid-to-cusp transition occuring apparently just above it (Tang, 1986; Pevtsov, 2002a; Gibson *et al.*, 2002). We will discuss the implications of this observed phenomenon further below.

Both S and inverse-S morphology are observed, but more S-shaped sigmoids are observed in the southern hemisphere, and more inverse-S shapes are observed in the northern hemisphere (Rust and Kumar, 1996; Pevtsov *et al.*, 2001). This is consistent with other observed patterns, such as a predominantly negative (left-handed) current helicity observed in the northern hemisphere, and positive (right-handed) in the southern hemisphere (Seehafer, 1990; Pevtsov *et al.*, 1995), as well as patterns of chirality in H-alpha filaments (Martin *et al.*, 1992; 1994). Thus, sigmoids are of interest because of their association with dynamic phenomena such as flares and CMEs, but also because they provide clues to the global organization of magnetic helicity, which is believed to be very nearly conserved as a global quantity in the highly conducting corona (Berger and Field, 1984).

2.2. Sigmoid as Flux Rope

With the advent of the Yohkoh soft-X-ray Telescope, the first comprehensive sigmoid studies were obtained (Manoharan *et al.*, 1996; Hudson *et al.*, 1998; Sterling and Hudson, 1997; Pevtsov and Canfield, 1999; Canfield *et al.*, 2000) and immediately it was suggested that they were manifestations of a magnetic flux rope topology (Rust and Kumar, 1996). Sheared magnetic field lines are intrinsically S-shaped, and the hemisphere rules of sigmoid direction are plausibly connected to the direction of magnetic helicity implied by other observations. Thus, a left (right)-handed magnetic flux rope should yield an inverse (forward) S-shaped soft-X-ray sigmoid. However, as Figure 1 demonstrates, both forward and inverse-S shapes are contained in a twisting field line, and simulations of flux ropes emerging into the corona generally contain both forward and inverse S-shaped field lines (Fan, 2001; Magara and Longcope, 2001; Fan and Gibson, 2003; Abbett *et al.*, 2003; Archontis *et al.*, 2004). In the case of Figure 1, the rope is left-handed, and the bottoms of the winding field lines are inverse-S shaped, while the tops are forward-S shaped. Thus, to be consistent with the observed hemispheric rules, sigmoids should be showing the bottoms, or dipped portions of sheared field lines.

It has been proposed that soft-X-ray sigmoids are the manifestations of flux ropes undergoing the kink instability. For example, the sigmoid could indicate the kinked axis of the flux rope (Rust and Kumar, 1996). Usually, however, if the axial field line is arched upwards when a left-handed flux rope kinks, the rope axis behaves as the tops of flux rope field lines and forms a forward-S shape (Fan and Gibson, 2003; 2004; Kliem *et al.*, 2004). Cases have been found where a left-handed rope's axis is dipped downwards and possesses an inverse-S shape (Magara and Longcope, 2001; 2003) or where an originally upward-arched axial field line kinks downward as it undergoes the kink instability (Kliem *et al.*, 2004). However, if we wish to relate these or any other flux rope field lines to the soft-X-ray sigmoid, it is necessary to provide a physical reason why these particular dipped field lines are heated.

One potential heat source could be Joule heating in regions of enhanced currents. Török and Kliem (2003) and Aulanier *et al.* (2005a) found that as a line-tied flux rope is subjected to photospheric twisting motions, e.g. as might arise from sunspot rotation, the current density peaks in a sigmoid flux bundle in the bottom part of the twisting flux rope or in a current layer of sigmoid projected shape (of correct direction) below the flux rope. Since these structures exist both in quasi-steady and in erupting twisting flux ropes and since sunspot rotations may persist over periods of days (Brown *et al.*, 2003), such ropes or current layers might give rise to either persistent or transient sigmoids. However, it remains to be shown that the current density steepens sufficiently in this system so that the energy requirement of the sigmoid soft-X-ray emission would be met.

2.3. Sigmoid Due to Heating at Current Sheets

Electric current sheets are regions where the magnetic field is discontinuous across very thin spatial scales, and, generally speaking, the thinner the sheet, the stronger the current density. Such regions are thus good candidates for providing sufficient heating to raise sigmoid structures to soft-X-ray temperatures. The discontinuous magnetic fields at the current sheets can reconnect, and the thermal energy released by reconnecting magnetic fields is widely invoked to explain the required heating rate for soft-X-ray solar flares (Yokoyama and Shibata, 1998). In general, reconnections arising in numerical simulations such as will be discussed below result from numerical diffusion in regions of large gradients, and may not model realistic reconnection rates. 3D numerical simulations also tend not to explicitly model the dissipation processes which would heat the soft-X-ray loops. However, the locations of numerically-driven reconnections can have clear physical origins, e.g., current sheets. It is reasonable to consider where in a given magnetic topology current sheets would be likely to form. [In addition to the cases discussed below, see also Amari *et al.* (2000) and Kusano (2005) for examples of how reconnecting sigmoid field lines might arise during the (noneruptive) formation of flux ropes].

2.3.1. *Current Sheets at Interface of Rope and Ambient Field*

Current sheets are known to form at the boundary between a straight, cylindrically symmetric flux rope and its surrounding magnetic fields when it undergoes the kink instability (Rosenbluth *et al.*, 1973; Arber *et al.*, 1999; Gerrard *et al.*, 2001). An analogous helical current sheet can form around an arched flux rope that undergoes the kink instability. However, as discussed above, the forwards-S shape of this helical current sheet for a left-handed rope kinking upwards is inconsistent with sigmoid hemisphere rules. On the other hand, if such a left-handed rope kinks downwards instead of erupting upwards, the helical current sheet forms an inverse-S shape. Thus, one possible explanation for sigmoids could be heating along helical current sheets of downward kinking ropes (Kliem *et al.*, 2004).

2.3.2. *Current Sheets at Bald-Patch-Associated Separatrix Surface*

An alternative location for current sheet formation is a separatrix surface that arises because of line-tying at a rigid boundary, such as the photosphere (Parker, 1994; Titov and Demoulin, 1999, hereafter T&D; Low and Berger, 2003). Figure 3 shows a set of dipped field lines which form such a surface within a left-handed flux rope, and which possess the correct sigmoid direction (inverse-S). The bald patch (BP) of a coronal magnetic field structure is defined as the locus of points where dipped field just touches the photosphere (i.e. at the centers of the purple field lines shown in Figure 3). The bald-patch-associated separatrix surface (BPSS) is made up of the field lines that contain the BP points. Magnetic connectivity is discontinuous across the BPSS, because the field lines are line-tied to the (assumed) rigid photosphere. Dynamic evolution of the flux rope field lying above and within this separatrix surface relative to the shorter, arcade-type field below and external to it, could result in tangential discontinuities, leading to the the formation of electric current sheets along this sigmoid separatrix surface.

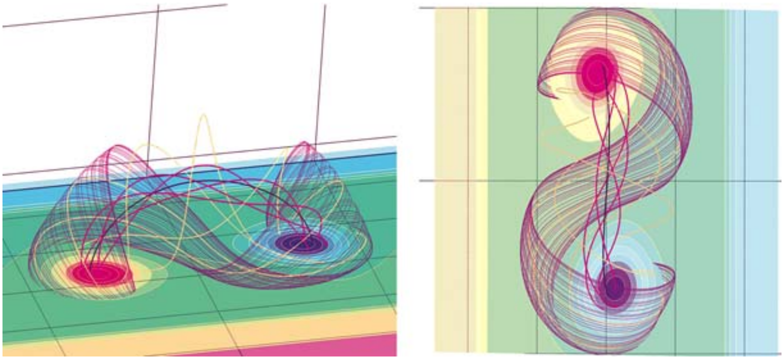

Figure 3. Bald-patch-associated separatrix surface (BPSS) (group of purple field lines) overlaid on sample flux-rope field lines for Fan and Gibson (2003; 2004) simulation time step 39. Color contours at lower boundary represent normal magnetic field at the photosphere. From Gibson *et al.* (2004).

2.3.3. *Current Sheets at Magnetic X-Line*

A well-studied location for current sheets to occur is in the region of magnetic X-points, and in three dimensions we can generalize this to a magnetic X-line along which the poloidal field comes to an X-point (the axial component of the field is not necessarily zero) (see e.g. Gorbachev and Somov, 1988). Such an X-type magnetic topology can exist below the flux rope instead of or in addition to a BPSS (see Section 4). In the classical picture of an eruptive flare, a vertical current sheet is formed behind an erupting flux rope where oppositely directed field lines reconnect to form the detached rope plasmoid with arcade field below (e.g. Anzer and Pneuman, 1982; Yokoyama and Shibata, 1998). More generally, this X-line could pinch into a current sheet under very general, possibly small perturbations (Titov *et al.*, 2003; Galsgaard *et al.*, 2003; Aulanier *et al.*, 2005b). Thus, as in the case of a BPSS, any type of perturbation of such configurations might be expected to light up sigmoid field lines reconnecting at the current sheets forming in the vicinity of the X-line.

3. Dynamic Perturbations

The question we are faced with is, what could cause dynamic perturbations of a flux rope and lead to current sheet formation and heating along sigmoid field lines? In this section we will briefly discuss some possibilities, which together can explain the range of observed sigmoids, from transient to persistent.

3.1. Eruptive Perturbations of Flux Ropes

In two related simulations, Fan and Gibson (2003; 2004) and Török *et al.* (2004) demonstrated that a flux rope in a coronal atmosphere underwent the kink instability

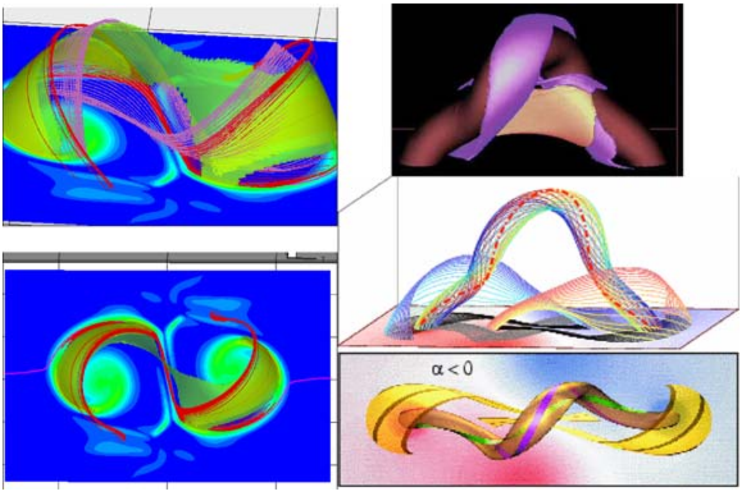

Figure 4. (Left bottom) Comparison of Fan and Gibson (2003; 2004) $t = 56$ BPSS (red field lines) to current sheets (yellowish-green isosurfaces), and (left top) same, with $t = 39$ BP-associated separatrix surface also shown (purple field lines) (both figures from Gibson *et al.*, 2004). (Right top) Vertical current sheet forming in the vicinity of magnetic X-line (yellow isosurface) during flux rope eruption (Török *et al.*, 2004). (Right middle) Field lines associated with this eruption, including two sets (red and blue) that intersect vertical current sheet, and (right bottom) same field lines seen from top (from Kliem *et al.*, 2004).

and erupted as it crossed a threshold for magnetic twist. Note that by "eruption" we mean a significant sudden upward motion, not necessarily implying an ejection of material from the corona. In both of these simulations, the left-handed flux rope axis kinked into a forwards S, inconsistent with observed hemispheric trends.

In the simulation of Fan and Gibson (2003; 2004), current sheets formed in the correct shape of an inverse S, and Gibson *et al.* (2004) demonstrated that these current sheets indeed formed along the BPSS as predicted (Figure 4, left). Thus the kink-instability-triggered eruption acted as a strong dynamic perturbation of the BPSS, creating a sharply defined, transient soft-X-ray sigmoid. Gibson and Fan (2006) analyzed the end-state of a related simulation (in spherical coordinates, see e.g. Fan, 2005), which resulted in the ejection of the upper part of the flux rope. They found that a vertical current sheet formed behind the ejecting portion of the flux rope (Figure 5 left) and cusped field lines closed down via reconnection along this current sheet (Figure 5 middle), as in the classical model of eruptive flares.

In the Török *et al.* (2004) simulation, the magnetic topology differed in that there was an X-line rather than a BPSS. We will discuss the reasons for and implications of this difference in greater detail below. In this analysis, a vertical current sheet formed beneath the erupting flux rope in the vicinity of the X-line. (Figure 4 right, top). Kliem *et al.* (2004) demonstrated that if one traced field lines passing close to this current sheet, they formed a sigmoid shape in the correct direction for

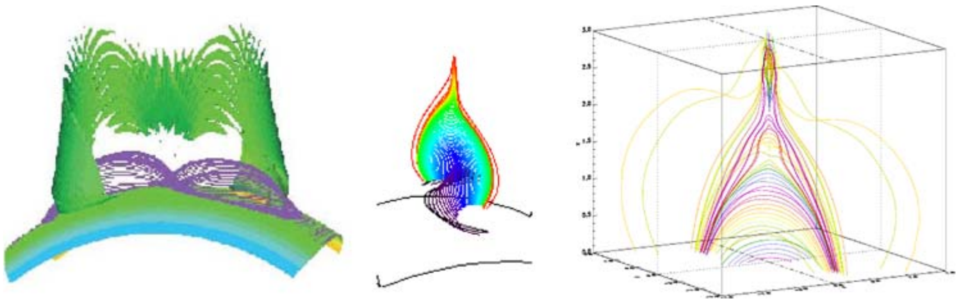

Figure 5. End-states: (left) Vertical current sheet forming behind portion of flux rope that escapes and (middle) cusp-shaped field lines reconnecting below erupting rope (Gibson and Fan, 2006). (Right) Cusped field lines reconnecting below erupting rope (Török and Kliem, 2005). Not all of the twisted rope has erupted in the Gibson and Fan (2006) case: a sigmoid BPSS is still present beneath the reconnecting field (left and middle frames).

the direction of magnetic twist (Figure 4 right, middle and bottom). As in the Fan (2005) simulation, cusped field lines were found beneath another, related simulated erupting flux rope in which the flux rope was ejected (Török and Kliem, 2005) (Figure 5, right).

Both the Gibson and Fan (2006) and the Török and Kliem (2005) results are consistent with a transient sigmoid brightening transitioning to a soft-X-ray cusp as in Figure 2. One difference between these two simulations, however, is that Gibson and Fan (2006) demonstrated the continued presence of a flux rope lying below the post-flare loops, as evidenced by the BPSS present in the left and middle frames of Figure 5. We will discuss the consequences of such a partly-expelled flux rope in more detail below.

3.2. Noneruptive Perturbations of Flux Ropes

As discussed in Section 2, any dynamic perturbation could cause current sheet formation along the BPSS or in the vicinity of the X-line. Indeed, Török *et al.* (2004) found that the X-line pinched into a current sheet even during the relaxation of the approximate analytical equilibrium of Titov and Demoulin (1999, hereafter T&D) to a nearby stable numerical equilibrium. Similarly, Fan and Gibson (2006) found that, even during the quasistatic evolution of the a confined flux rope before its eruption, sigmoid current sheets formed along the BPSS. These topologies present a "fault line" in the coronal magnetic field across which field lines behave very differently when driven dynamically. Thus, many different perturbations, ranging from flux emergence to photospheric motions at the footpoints of the field lines, may constantly cause the development of magnetic tangential discontinuities (or current sheets) where reconnections heat persistent, or long-lived sigmoids.

For example, the dynamic emergence of the flux rope from below the photosphere into the corona is a possible physical driver of current sheet formation at the BPSS. Dense photospheric material weighing down the dipped field prevents easy emergence when this is simulated (Fan, 2001; Magara and Longcope, 2001, 2003). However, as more axial flux is transported upward by the Lorentz-force induced shear, a sigmoid current sheet forms and reconnection allows the dipped field to lose some of its anchoring mass and emerge into the corona (Manchester *et al.*, 2004b). Depending upon whether this is a continuous process or one that occurs in fits and starts, it could result in either the continuous heating of a persistent sigmoid, or a series of transient sigmoids.

Cases where the flux rope kinks but does not erupt might also drive sigmoid heating. Fan and Gibson (2006) demonstrated such a case where a less twisted flux rope reached a stable equilibrium with a somewhat kinked axis, and indeed current sheets formed along the BPSS during this writhing motion. In another example, as mentioned above, Kliem *et al.* (2004) described a case where a downward kinking left-handed rope formed an inverse-S-shaped, helical current sheet at its interface with surrounding magnetic fields. These scenarios are then consistent with reconnection heating forming a transient, but non-CME related sigmoid.

4. Partly vs. Fully Expelled Flux Ropes

The degree to which the flux rope is expelled may depend upon whether reconnections occur behind or within the rope, and this in turn may depend upon whether or not the flux rope lies down low enough in the corona to possess a BPSS. Figures 6 and 7 illustrate this point in 2D and 3D respectively. Figure 6 shows 2D cartoons of a flux rope viewed along its axis. If reconnection occurs at an X-point below the flux rope (left), it can be completely expelled. If reconnection occurs within the flux rope (right), some of the rope remains behind and it is partly expelled.

Figure 7 demonstrates this in 3D. The flux rope shown in this image is based on the T&D model, an analytic model of a flux rope within an arcade field. When the T&D model flux rope is only partly "emerged" above the photosphere so that there is a single, continuous BP of dipped field grazing the central portion of the neutral line (left image), there is a corresponding single BPSS. This configuration is very similar to that of Fan and Gibson (2003; 2004), and is the 3D analogue to the right-hand images of Figure 6. Such a configuration is shown in Gibson and Fan (2006) to lead to partial rope expulsion, with a BPSS left behind. In this case there is no magnetic X-line before the eruption, but reconnection occurs as opposing upper portions of BPSS field lines are squeezed together when the flux rope axis kinks. The lower portions of these same field lines reconnect to form the lower, remaining flux rope BPSS shown in Figure 5.

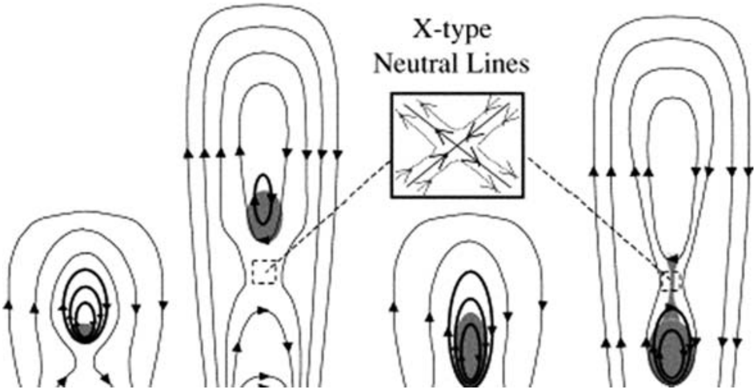

Figure 6. Cartoons of erupting flux ropes, viewed along their axes. (Left) Reconnection occurring at the X point below the rope, leading to the total expulsion of the flux rope and prominence. (Right) Reconnection occurring within the flux rope and prominence, leading to the partial expulsion of the flux rope and prominence. Adapted from Gilbert *et al*. (2001).

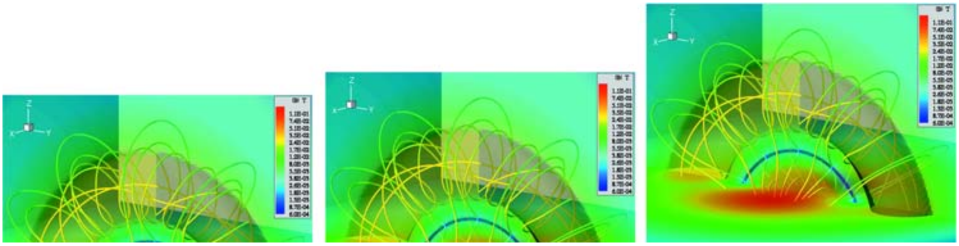

Figure 7. T&D-type flux rope at various stages of "emergence". (Left) Low enough in the coronal atmosphere so that there is no X-line, but the T&D rope would have a single BPSS. (Middle) Higher in the atmosphere, so that the X-line (blue line) is present, and the BPSS would be bifurcated. (Right) High enough to have an X-line but no BPSS in the T&D rope. Note that the images shown are adapted from Roussev *et al*. (2003), and show a version of the T&D model with purely poloidal field outside the rope, so the comments regarding BPSSs made here should be taken with regards to the analogous stage of "emergence" of the true T&D model, which does have finite twist outside the rope.

If the axis of the flux rope lies high enough in the atmosphere, the magnetic X-line will be present and the BPs will either bifurcate into two (middle image), or disappear altogether if the curvature of the rope legs is such that no concave-up fields intersect the photospheric neutral line (right image: see Titov and Demoulin (1999) for discussion). The Török and Kliem (2005) simulation uses the T&D model with no BP as its starting point, and demonstrates how a flux rope can be expelled essentially in entirety during eruption, reconnecting in the vicinity of the magnetic X-line and leaving behind cusped, post-flare fields.

4.1. Observational Consequences of Partly-Expelled Flux Rope

4.1.1. *Partial Filament Eruptions*

Since the partly-expelled flux rope leaves behind a BPSS, a sigmoid could reform soon after an eruption. It also explains how a filament might partially erupt, or even be unperturbed by the flux rope eruption as has been observed (Tang, 1986; Pevtsov, 2002a; Gibson *et al.*, 2002). The filament is expected to lie within the dips of the magnetic flux rope, and so a BPSS-sigmoid would wrap around it, with loop apexes lying above it (see Figure 3). When modeled this way observations of related quiescent filaments and persistent sigmoids are well-matched (Gibson *et al.*, 2004). Referring to Figure 6 again, we see that depending on where the reconnection happens, the filament will partially erupt, or not erupt at all (Gilbert *et al.*, 2001). As the eruption begins, the BPSS is dynamically forced, causing a transient sigmoid brightening. Gibson and Fan (2006) demonstrated that the kinking rope's legs then are squeezed together, creating a vertical current sheet where sigmoid field lines reconnect, breaking the rope in two. As the eruption continues, the field-lines reconnecting at the vertical current sheet become less sigmoid-shaped, and more cusp-shaped, closing down above the surviving dipped, possibly filament-containing field which is essentially unaffected by the eruption.

4.1.2. *Relevance for Magnetic Cloud Observations*

Magnetic clouds, known to be associated with CMEs and filament eruptions, can be examined for evidence of entrained, cool, filament material, by examining the charge states of solar wind ions within them which are "frozen in" at coronal temperatures. Such analyses of magnetic clouds tend to indicate only relatively hot coronal material. However, some cases have been found (He^{+} events) that imply cool material coexisting with hot material (Skoug *et al.*, 1999; Gloeckler *et al.*, 1999). One recent case (Zurbuchen *et al.*, 2005) (Jan 9–10, 2005) demonstrates purely cold material, and it is worth noting that this event had no associated flare.

It has been argued that the coronal temperature diagnostics provided by magnetic clouds may be able to help distinguish between different eruption models (Lynch *et al.*, 2004). For example, if the filament contained in a pre-CME flux rope were to erupt without reconnections, it should result in the presence of cool magnetic cloud material, whereas if a flux rope were formed via reconnections during eruption, any entrained filament material would be heated. However, we have demonstrated that in a partly-expelled flux rope, filament-entrained field lines can also experience reconnections and heating. Indeed, Figure 6 demonstrates that all, some, or none of the filament-carrying field lines might undergo reconnections during a flux rope eruption, making it tempting to speculate that all three types of magnetic clouds (hot, mixed, or cool) might arise. We hesitate to go this far, since we feel that equating the heated magnetic cloud material with localized reconnections during eruption is likely to be an oversimplification. However, we do assert that the internal reconnections during the partial eruption of a pre-existing flux rope (or for that matter, the reconnections between an erupting flux rope and external field (Amari *et al.*, 2003b)), are as likely to heat entrained filament material as reconnections that occur when a rope is formed during eruption.

5. Conclusions

The combined results presented here demonstrate that sigmoid evolution, before, during, and after a CME, is consistent with the presence of a long-lived coronal magnetic flux rope. Before any CME occurs, the sigmoid can appear as a general brightening possessing an S or inverse-S pattern, for example during the more-or-less continuous dynamic perturbation of field lines at the BPSS or in the vicinity of an X-line. During the CME, transient sigmoids might occur as the rope loses equilibrium and erupts, causing current sheet formation along the BPSS or again at the X-line. During and after the CME, field lines reconnect into cusped field lines below the erupting portion of the rope in accordance with the observed transition of the transient sigmoid into a cusp. If the flux rope is only partly expelled, the BPSS may remain, allowing a quick return to persistent or transient soft-X-ray sigmoids, or indeed eventually to more eruptions. A partly-expelled flux rope could also explain partially or non-erupting filaments, as well as the presence of hot or mixed temperature charge states within magnetic clouds.

Acknowledgements

S.E.G. wishes to thank all the ISSI workshop participants for an excellent tutorial on the integrated solar-heliosphere-magnetosphere system, and T. Zurbuchen in particular for discussions on magnetic cloud charge states. She also thanks J. Goldstein and B. T. Klöun for their animated debates at the workshop. We thank H. Gilbert and I. Roussev for permitting us to adapt their figures, and T. Holzer and an anonymous referee for helpful comments. T.T. and B. K. thank the John von Neumann-Institut for Computing, Jülich for computer time. S. E. G. and Y. F. were supported in part by AFOSR grant F49620-02-0191, and B. K. was supported by DFG grant MA 1376/16-2. The Yohkoh SXT project is a collaborative project of LMSAL, the National Astronomical Observatory of Japan, and the University of Tokyo, supported by NASA and ISAS.

References

Abbett, W. P., and Fisher, G. H.: 2003, *Astrophys. Journ.* **582**, 475.
Anzer, U., and Pneuman, G. W.: 1982, *Solar Phys.* **79**, 129.
Amari, T. *et al.*: 2000, *Astrophys. Journ.* **529**, L49.

Amari, T. *et al.*: 2003a, *Astrophys. Journ.* **585**, 1073.
Amari, T. *et al.*: 2003b, *Astrophys. Journ.* **95**, 1231.
Arber, T. D., Longbottom, A. W., and van der Linden, R. A. M.: 1999, *Astrophys. Journ.* **517**, 990.
Archontis, V. *et al.*: 2004, *Astron. and Astrophys.* **426**, 1047.
Aulanier, G., Démoulin, P., and Grappin, R.: 2005a, *A&A* **430**, 1067.
Aulanier, G., Pariat, E., and Démoulin, P.: 2005b, *A&A* **444**, 961.
Berger, M. A., and Field, G. B.: 1984, *J. Fluid Mech.* **147**, 133.
Brown, D. S. *et al.*: 2003, *Solar Phys.* **216**, 79.
Burlaga, L. *et al.*: 1982, *Geophys. Res. Lett.* **9**, 1317.
Canfield, R. C., Hudson, H. S., and Pevtsov, A. A.: 2000, *IEEE Trans. Plasma Sci.* **28**, 1786.
Chen, J., and Krall, J.: 2003, *Journ. Geophys. Res.* **108**, CiteID 14010.
Fan, Y.: 2005, *Astrophys. Journ.* **630**, 543.
Fan, Y.: 2001, *Astrophys. Journ.* **554**, L111.
Fan, Y., and Gibson, S. E.: 2006, *ApJL* **641**, L149.
Fan, Y., and Gibson, S. E.: 2004, *Astrophys. Journ.* **609**, 1123.
Fan, Y., and Gibson, S. E.: 2003, *Astrophys. Journ. Lett.* **589**, L505.
Galsgaard, K., Titov, V. S., and Neukirch, T.: 2003, *ApJ* **595**, 506.
Gerrard, C. L., Arber, T. D., Hood, A. W., and van der Linden, R. A. M.: 2001, *Astron. and Astrophys.* **373**, 1089.
Gibson, S. E., and Fan, Y.: 2006, *ApJL* **637**, L65.
Gibson, S. E. *et al.*: 2004, *Astrophys. Journ.* **617**, 600.
Gibson, S. E. *et al.*, 2002, *Astrophys. Journ.* **574**, 1021.
Gilbert, H. R., Holzer, T. E., Low, B. C., and Burkepile, J. T.: 2000, *Astrophys. Journ.* **549**, 1221.
Gorbachev, V. S., and Somov, B. V.: 1988, *Solar Phys.* **117**, 77.
Gloeckler, G. *et al.*: 1999, *Geophys. Res. Lett.* **26**, 157.
Hagyard, M. J., Teuber, D., West, E. A., and Smith, J. B.: 1984, *Solar Phys.* **91**, 115.
Hudson, H. S. *et al.*: 1998, *Geophys. Res. Lett.* **25**, 248.
Kliem, B., Titov, V. S., and Török, T.: 2004, *Astron. and Astrophys.* **413**, L23.
Kusano, K.: 2005, *Astrophys. Journ.* **631**, 1260.
Leka, K. D., Canfield, R. C., McClymont, A. N., and van Driel-Gesztelyi, L.: 1996, *Astrophys. Journ.* **462**, 547.
Lites, B. W. *et al.*: 1995, *Astrophys. Journ.* **446**, 877.
Lites, B. W., and Low, B. C.: 1997, *Solar Phys.* **174**, 91.
Low, B. C.: 1996, *Solar Physics* **167**, 217.
Low, B. C., and Berger, M.: 2003 *Astrophys. Journ.* **589**, 644.
Lynch, B. J. *et al.*: 2004, *Astrophys. Journ.* **617**, 589.
MacNeice, P. *et al.*: 2004, *Astrophys. Journ.* **614**, 1028.
Magara, T., and Longcope, D.: 2003, *Astrophys. Journ.* **586**, 630.
Magara, T., and Longcope, D.: 2001, *Astrophys. Journ. Lett.* **559**, L55.
Manchester, W. *et al.*: 2004a, *Journ. Geophys. Res.* **109**, CiteID A01102.
Manchester, W., Gombosi, T., DeZeeuw, D., and Fan, Y.: 2004b, *Astrophys. Journ.* **610**, 588.
Manoharan, P. K., van Driel-Gesztelyi, L., Pick, M., and Demoulin, P.: 1996, *Astrophys. Journ. Lett.* **468**, L73.
Martin, S. F., Marquette, W. H., and Bilimoria, R.,1992, in K. Harvey (ed.), *ASP Conf. Proc. 27, The Solar Cycle*, (San Francisco: ASP), 53.
Martin, S. F., Bilimoria, R., and Tracadas, P. W.: 1994, in R. J. Rutten and C. J. Schrijver (eds.), (*NATO ASI Ser. C, 433*) Solar Surface Magnetism, (Dordrecht: Kluwer), 303.
Parker, E. N.: 1994, Spontaneous Current Sheets in Magnetic Fields, Oxford University Press, New York.
Pevtsov, A. A., Canfield, R. C., and Metcalf, T. R.: 1995, *ApJ* **440**, L109.

Pevtsov, A. A., Canfield, R. C., and Zirin, H.: 1996, *Astrophys. Journ.* **473**, 533.
Pevtsov, A. A., and Canfield, R. C.: 1999, Magnetic Helicity in Space and Laboratory Plasmas, in M. R., Brown, R. C. Canfield, and A. A. Pevtsov, (eds.), *Geophys. Monogr. Ser., AGU*, Washington D. C., vol. 111, 103.
Pevtsov, A. A., Canfield, R. C., and Latushko, S. M.: 2001, *Astrophys. Journ. Lett.* **549**, L261.
Pevtsov, A. A.: 2002, *Sol. Phys.* **207**, 111.
Pevtsov, A. A.: 2002, Yohkoh 10th Anniversary Meeting Proceedings, eds. Martens and Cauffman, COSPAR Colloquia Series, Elsevier, 125.
Rosenbluth, M. N., Dagazian, R. Y., and Rutherford, H. P.: 1973, *Phys. Fluids* **16**, 1894.
Roussev, I. I. *et al.*: 2003, *Astrophys. Journ.* **588**, L45.
Rust, D. M., and Kumar, A.: 1994, *Solar Phys.* **155**, 69.
Rust, D. M., and Kumar, A.: 1996, *Astrophys. Journ. Lett.* **464**, L199.
Rust, D. M.: 2003, *Adv. in Space Res.* **32**, 1895.
Seehafer, N.: 1990, *Sol. Phys.* **125**, 219.
Skoug, R. *et al.*: 1999, *Geophys. Res. Lett.* **26**, 161.
Sterling, A. C., and Hudson H. S.: 1997, *Astrophys. Journ. Lett.* **491**, L55.
Tanaka, K.: 1991, *Sol. Phys.* **136**, 133.
Tang, F.: 1986, *Sol. Phys.* **105**, 399.
Titov, V. S., and Demoulin, P.: 1999, *Astron. Astrophys.* **351**, 70.
Titov, V. S., Galsgaard, K., and Neukirch, T.: 2003, *ApJ* **582**, 1172.
Török, T., and Kliem, B. 2003, *A&A* **406**, 1043.
Török, T., Kliem B., and Titov, V. S.: 2004, *Astron. and Astrophys.* **413**, L27.
Török, T., and Kliem, B.: 2005, *Astrophys. Journ. Lett.* **630**, L97.
Yokoyama, T., and Shibata, K.: 1998, *Astrophys. Journ. Lett.* **494**, L113.
Zurbuchen, T. H., *et al.*: 2005, AGU Spring meeting 2005, abstract SH54B-04.